1990ApJ...353..640L

THE ASTROPHYSICAL JOURNAL, 353:640–653, 1990 April 20
© 1990. The American Astronomical Society. All rights reserved. Printed in U.S.A.

HIGH-RESOLUTION SPECTROSCOPY OF THE C_2 SWAN 0–0 BAND FROM COMET P/HALLEY[1]

D. L. LAMBERT AND Y. SHEFFER
University of Texas at Austin

A. C. DANKS
Applied Research Corporation

C. ARPIGNY
Université de Liège

AND

P. MAGAIN
European Southern Observatory

Received 1989 August 25; accepted 1989 October 18

ABSTRACT

High-resolution ($\lambda/\Delta\lambda \simeq 80{,}000$) spectra of the C_2 Swan system's 0–0 band from comet P/Halley in 1986 March show that the populations of the upper ($d\ ^3\Pi_g$) state's rotational levels may be described by two rotational temperatures. The low rotational levels ($J' \lesssim 15$) provide a low temperature: $T_{rot} \sim 600$–700 K. The higher levels correspond to $\sim$3200 K. If a contribution from the "3200 K" molecules is subtracted from the populations of the low-J' levels, the latter are characterized by the low-temperature $T_{rot} \simeq 190$ K.

A comparison with recent predictions for C_2 molecules fluorescing in sunlight shows that the observed and predicted level populations are in good agreement for $J' \gtrsim 15$, but there is a sharp disagreement for the low rotational levels: the observations show that the $^3\Pi_0$, $^3\Pi_1$, and $^3\Pi_2$ substrates at low J' have very similar populations and an identical T_{rot} to within the errors of measurement, but, by contrast, the predictions give three quite different forms for the run of population with J' for these substates. It is argued that the addition of the previously overlooked satellite transitions within the Swan system to the fluorescence studies may reproduce the observed populations at low J' and yet leave unaffected the agreement between predicted and observed populations at high J'. It is also noted that the observed line fluxes may include a contribution from freshly formed molecules that have yet to achieve fluorescence equilibrium.

Subject headings: abundances — comets

I. INTRODUCTION

The cometary emission bands of the C_2 Swan ($d\ ^3\Pi_g$–$a\ ^3\Pi_u$) system result as C_2 molecules fluoresce in sunlight. Between their creation from a larger or parent molecule and their destruction by solar ultraviolet photons, the C_2 molecules fluoresce in the sunlight for about 10^5 s and attain statistical equilibrium well before they are photodissociated. Initial distributions of the molecules over the rovibronic levels of each electronic state are expected to be erased quickly. Prediction of the C_2 spectrum would seem to be a well-defined problem involving the known solar fluxes and a suite of molecular data.

In this paper, we present and discuss high-resolution spectra of comet P/Halley showing the rotational structure of the Swan system's 0–0 band from the *P*-branch band head at 5165.2 Å to near 5131 Å. The populations of the rotational levels in the lowest vibrational level of the $d\ ^3\Pi_g$ state are derived and qualitative comparisons made with predictions for C_2 molecules fluorescing in sunlight. Two surprising results are reported:

1. We find that the rotational populations cannot be described by a single rotational temperature. The lower rotational levels ($J' \lesssim 15$) provide a low-temperature $T_{rot} \sim 600$ to 700 K, but, for the higher levels, $T_{rot} \sim 3200$ K fits the derived populations. The higher temperature is characteristic of the vibrational temperatures previously reported for cometary C_2 molecules, e.g., $T_{vib} \simeq 3500$ K for comet West 1976 VI (Lambert and Danks 1983, hereafter LD) at a similar heliocentric distance.

2. For $J' \gtrsim 30$, the $^3\Pi_0$ or F_3 levels are underpopulated by a factor of about 1.3 relative to the mean of the $^3\Pi_2(F_1)$ and $^3\Pi_1(F_2)$ levels. In addition, the $^3\Pi_2$ levels are shown to be overpopulated relative to the $^3\Pi_1$ levels for $J' \simeq 30$–40.

II. OBSERVATIONS

Comet P/Halley was observed in 1986 March and April at the European Southern Observatory using the 1.4 m Coudé Auxiliary Telescope (CAT) and its coudé echelle spectrometer equipped with a 1872 diode Reticon array. The interval 5131–5170 Å was observed at resolutions of $\lambda/\Delta\lambda = 100{,}000$ (March 10) or 80,000 (March 24–30) with a dispersion of 0.023 Å per diode. Our observing log is summarized in Table 1. The spectrometer's entrance slit, which corresponded to 2″ by 20″ on the sky, was centered visually on the brightest portion of the diffuse cometary coma. Due to the low contrast of the image provided by the slit-viewing TV camera, the slit's precise position relative to the comet's nucleus is unknown. In addition to the usual sequence of flat-field lamp exposures to remove the diode-to-diode variations across the array, we observed Mars and the early-type star σ Sgr. An accurate wavelength calibration was obtained from a spectrum of a thorium-argon hollow cathode lamp. An acetylene torch observed with the

[1] Based on observations collected at the European Southern Observatory, La Silla, Chile.

© American Astronomical Society • Provided by the NASA Astrophysics Data System

1990ApJ...353..640L

TABLE 1

OBSERVING LOG

Date (UT) (1986)	r(AU)[a]	Δ(AU)[b]	Exposures
Mar 10.4.....	0.85	1.05	1 × 45 minutes
Mar 24.4.....	1.06	0.70	1 × 150 minutes
Mar 26.4.....	1.09	0.65	1 × 40 minutes, 1 × 45 minutes
Mar 27.3.....	1.10	0.63	3 × 60 minutes
Mar 28.4.....	1.12	0.60	1 × 60 minutes, 2 × 50 minutes
Mar 29.3.....	1.14	0.58	3 × 60 minutes
Mar 30.4.....	1.15	0.56	1 × 50 minutes, 2 × 60 minutes
Apr 8.19	1.29	0.43	30 minutes on nucleus
Apr 8.24	1.29	0.43	30 minutes at 20″ from nucleus toward Sun
Apr 8.27	1.29	0.43	30 minutes at 20″ from nucleus away from Sun
Apr 8.33	1.29	0.43	2 × 30 minutes at 40″ from nucleus toward Sun
Apr 8.39	1.29	0.43	30 minutes at 40″ from nucleus away from Sun

[a] Heliocentric distance of P/Halley.
[b] Geocentric distance of P/Halley.

same instrumental set-up provided intense Swan system lines at a rotational temperature apparently comparable to that of the comet's C_2 molecules.

Spectra of the several sources were reduced in the usual way: the fixed pattern signal was subtracted and the diode-to-diode variations were removed through division by the spectrum of the flat-field lamp. The cometary spectrum is contaminated by a reflected solar spectrum due to cometary dust. This contamination is readily removed using the Martian spectrum which is normalized and shifted to match the comet's spectrum longward of the 0–0 band head. This latter interval contains the strong Mg I *b* lines. Close inspection of the comet's spectrum before and after the subtraction of the scattered sunlight shows that the procedure is successful. The flux in the reflected solar spectrum was about 10% of the peak flux in the 5165 Å band head. Since the flat-field lamp and objects viewed through the CAT may not illuminate the spectrometer in identical fashions, we observed an early-type star (σ Sgr) to provide a flux calibration of the cometary spectrum. All cometary spectra shown here are ratios of P/Halley to σ Sgr, but our major conclusion concerning the rotational populations is unchanged if the ratios of P/Halley to the flat-field lamp are adopted. The ratio of the spectra of σ Sgr and the flat-field lamp varies almost linearly by 15% over the bandpass.

In order to enhance the signal-to-noise (S/N) ratio, individual spectra from a single night were co-added. A few obvious sharp blemishes introduced by bad diodes in the array or detected cosmic rays were removed and replaced by a mean value based on the signal in the adjacent diodes. Mean spectra from separate nights were added in various combinations. All of our major conclusions about the rotational temperatures of the $d\ ^3\Pi_g$ state are supported by the individual spectra. Figures

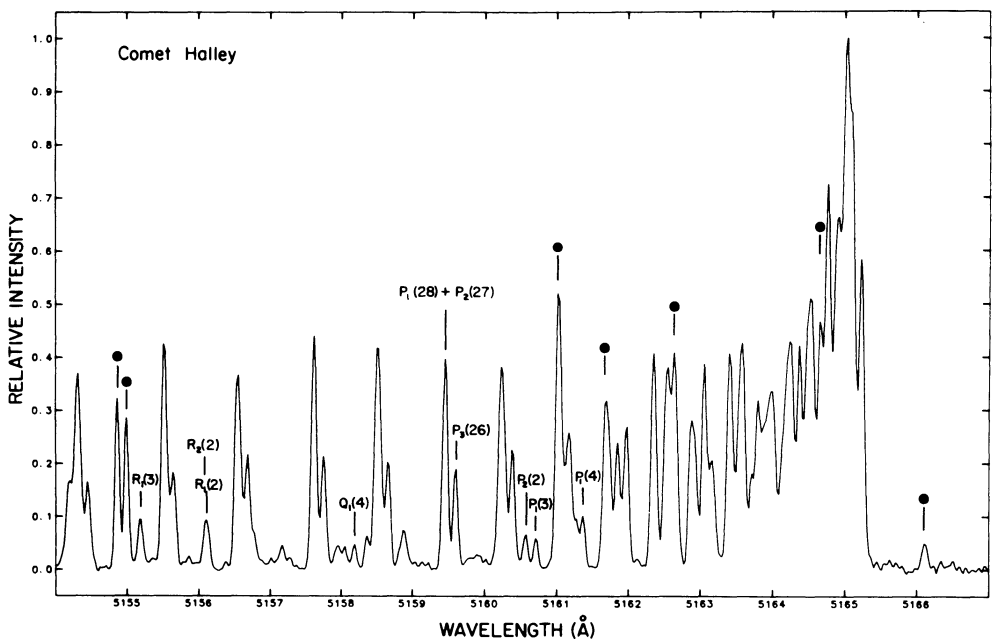

FIG. 1.—A portion of the observed spectrum of the 0–0 Swan band in comet Halley showing the *P*-branch band head. Selected C_2 lines are identified. Seven NH_2 lines including a weak line beyond the C_2 band head are identified by the filled circle above the marker locating a NH_2 line's wavelength.

© American Astronomical Society • Provided by the NASA Astrophysics Data System

1990ApJ...353..640L

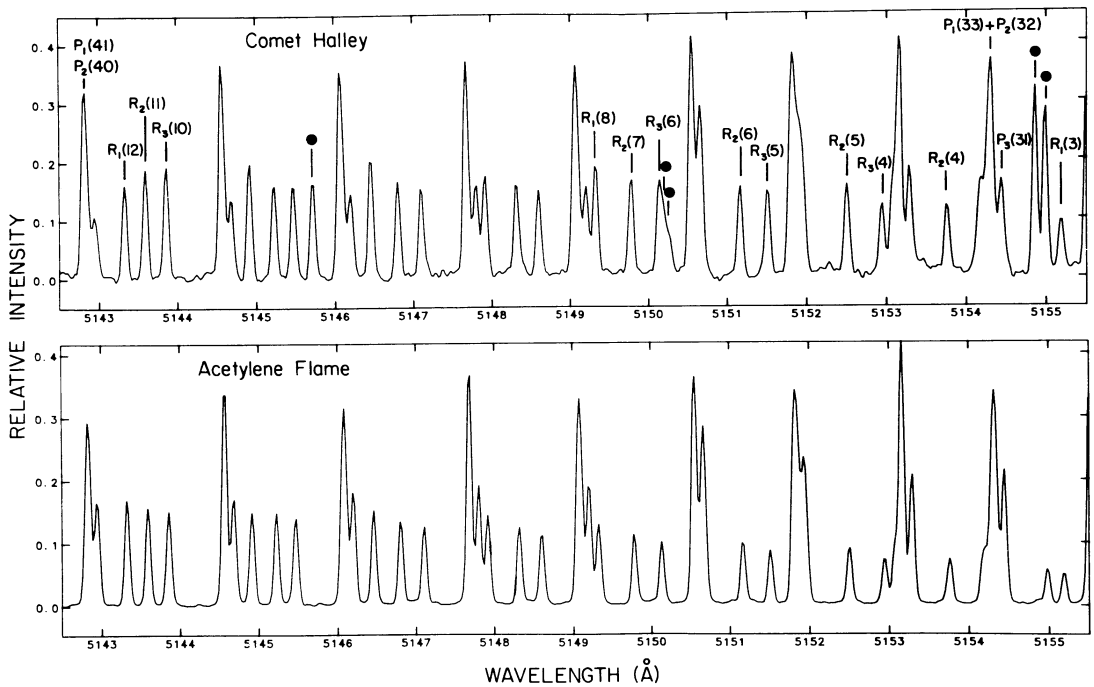

FIG. 2.—Portions of the observed spectrum of the 0–0 Swan band in comet Halley (*top panel*) and an acetylene flame (*bottom panel*). Selected C_2 lines are identified. Five NH_2 lines in the spectrum of comet Halley are identified by the filled circle above the marker locating a NH_2 line's wavelength. The flux scales of the two spectra were adjusted so that the *P*-branch lines have the same height in the figures. Then, the distinctly higher fluxes of the low-J' *R*-branch lines in the comet relative to the flame are obvious, as are the lower fluxes of the cometary P_3 lines.

1, 2, and 3 show the cometary emission spectrum that is provided by a co-addition of the set of high-resolution spectra from March 10 to March 30.

The widths (FWHM) of unblended lines in the spectrum of the comet and the acetylene torch are 76 ± 4 and 78 ± 2 mÅ, respectively. Such widths correspond to a resolution $\lambda/\Delta\lambda \simeq 67{,}000$ which is very slightly inferior to the nominal resolution ($= 80{,}000$ for all but one night) that is confirmed by the slightly narrower width (FWHM $= 64.2 \pm 0.7$ mÅ) of the thorium lines with very narrow (~ 7 mÅ) intrinsic widths. The measured FWHMs of cometary lines show that the process of co-addition of the nightly spectra has not resulted in significant smearing of the line profiles. The excess broadening over the instrumental width suggests internal motions of less than about 2 km s^{-1} within the observed line of sight through the comet.

On April 8, lower resolution spectra of the C_2 0–0 band were obtained at several positions across the comet—see Table 1. The entrance slit was set to provide a resolution $\lambda/\Delta\lambda = 20{,}000$ and corresponded to an area of 8″ by 20″ on the sky. In the sequence of 30 minute observations of the comet, the center of the slit was placed on the nucleus and then displaced 20″ and 40″ from the nucleus in the direction of the Sun and, then, in the direction of the comet's tail.

III. THE ROTATIONAL TEMPERATURE

Previous attempts to extract the excitation temperature of the $d\ ^3\Pi_g$ vibration-rotation levels from cometary Swan band spectra have used either integrated band fluxes to obtain a vibrational temperature from low-resolution spectra or synthetic spectra to extract vibrational and rotational temperature from medium- to high-resolution spectra. Since many C_2 lines are well resolved in our spectra, we elected to extract a rotational temperature using the integrated line fluxes (F_λ). When two C_2 lines are irretrievably blended, we use the total flux as long as the lines have nearly identical excitation energies, as happens with the unresolved pairs of $P_1(J+1) + P_2(J)$ lines. For optically thin emission lines from a single vibrational band (here v'–$v'' \equiv 0$–0),

$$F_\lambda \propto \frac{S_{J'J''}}{\lambda^4} \exp\left(-\frac{E_{v'J'}}{kT_{\rm exc}}\right),$$

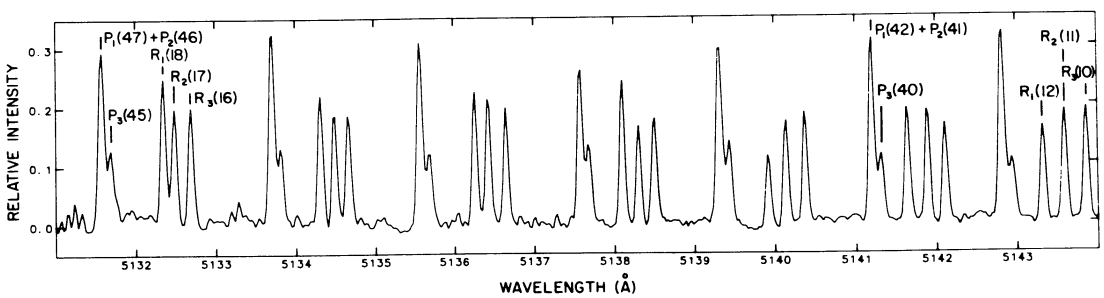

FIG. 3.—The last portion of the observed spectrum of the 0–0 Swan band in comet Halley. Selected C_2 lines are identified.

© American Astronomical Society • Provided by the NASA Astrophysics Data System

1990ApJ...353..640L

where λ is the wavelength of the transition from level (v', J') in $d\ ^3\Pi_g$ to level (v'', J'') in $a\ ^3\Pi_u$, $E_{v'J'}$ is the excitation energy of level (v', J'), $S_{J'J''}$ is the Hönl-London (rotational line intensity) factor, and T_{exc} is the excitation temperature as given by the population of level (v', J') relative to a reference level. We present the results of our measurements in the conventional form: a plot of $y = \log \lambda^4 F_\lambda / S_{J'J''}$ versus $E_{v'J'}$ (in cm^{-1}), where $y \propto N(v', J')/(2J' + 1)$ and $N(v', J')$ is the column density of molecules in the level (v', J'). For levels described by a single value of T_{exc} (in K), the reduced measurements y define a straight line with a slope of $-0.625/T_{exc}$. We refer to T_{exc} as the rotational temperature T_{rot} for $v' = 0$.

The fluxes F_λ were measured off the cometary spectra corrected for the reflected sunlight. In Table 2, we give relative fluxes for C_2 lines/blends. A few lines are omitted because they are blended with NH_2 lines (Dressler and Ramsay 1959). The wavelengths of the C_2 P and R lines are taken from Amiot (1983). For the low-J Q_1 and Q_2 lines, wavelengths were predicted from the molecular constants tabulated by Phillips (1968), and small empirical corrections were applied to these predictions using the differences between the predicted and observed P and R lines. The excitation energies ($E' \equiv E_{v'J'}$) were also computed from Phillips' molecular constants; the reference level is the lowest level ($v' = 0$, $J = 0$) of the ground ($X\ ^1\Sigma_g^+$) electronic state. Hönl-London factors ($S_{J'J''}$) were computed using a program written by Whiting (1973); the effect of the vibration-rotation interaction on $S_{J'J''}$ is negligible for the lines considered here (Dwivedi *et al.* 1978).

Solutions for T_{rot} were obtained from the mean spectra for each of the days on which high-resolution spectra were obtained. Since there are no major differences between the results for the separate days, we discuss the mean spectrum from the combined spectra. A novel result of these observations is that the line fluxes in Table 2 are not fitted by a single value of T_{rot}. This is quite evident in Figure 4. For $J' \lesssim 13$, the R-branch lines and a few P- and Q-branch lines yield to a low rotational temperature $T_{rot} = 665 \pm 70$ K and, within the limited line list, there is no evidence for population differences between $^3\Pi_0$, $^3\Pi_1$, and $^3\Pi_2$ or between the even- and odd-J levels. The higher J levels are clearly not fitted by an extrapolation of this "cold" population. In Figure 4, there appears to be a transition around $J' = 12$ from the low-T_{rot} to the high-T_{rot} populations. For $J' \gtrsim 15$, a rotational temperature around 3000 K is found. The fluxes of the $P_1 + P_2$ blends and the P_3 lines show that the F_3 ($^3\Pi_0$) levels are underpopulated relative to the mean of the F_1($^3\Pi_2$) and F_2($^3\Pi_1$) levels. Least-squares fits to the P-branch lines for $J' > 20$ give $T_{rot} = 3330 \pm 170$ K for the $P_1 + P_2$ blends and $T_{rot} = 2260 \pm 160$ K for the P_3 lines. Odd- and even-J' levels define the same relations to within the scatter of the individual points. This scatter, which is larger than the estimated errors of measurements, presumably arises from the effects of Fraunhofer lines on the excitation rates from $a\ ^3\Pi_u$ to $d\ ^3\Pi_g$. These formal solutions for T_{rot} consider lines over a relatively narrow interval in J'. Alternative interpretations are possible. For example, the mean population of F_1 and F_2 and the population of F_3 for $J' \gtrsim 35$ may have a similar T_{rot} ($\simeq 3300$ K) with F_3 underpopulated by a factor of 1.3 relative to the mean of F_1 and F_2. The hint in our data that the rotational temperature may be higher for the highest observed levels ($J' \simeq 39$–46) may reflect the well-known perturbation in the $v' = 0$ level of $d\ ^3\Pi_g$ at $N' = 34$ (Callomon and Gilby 1963; Amiot 1983).

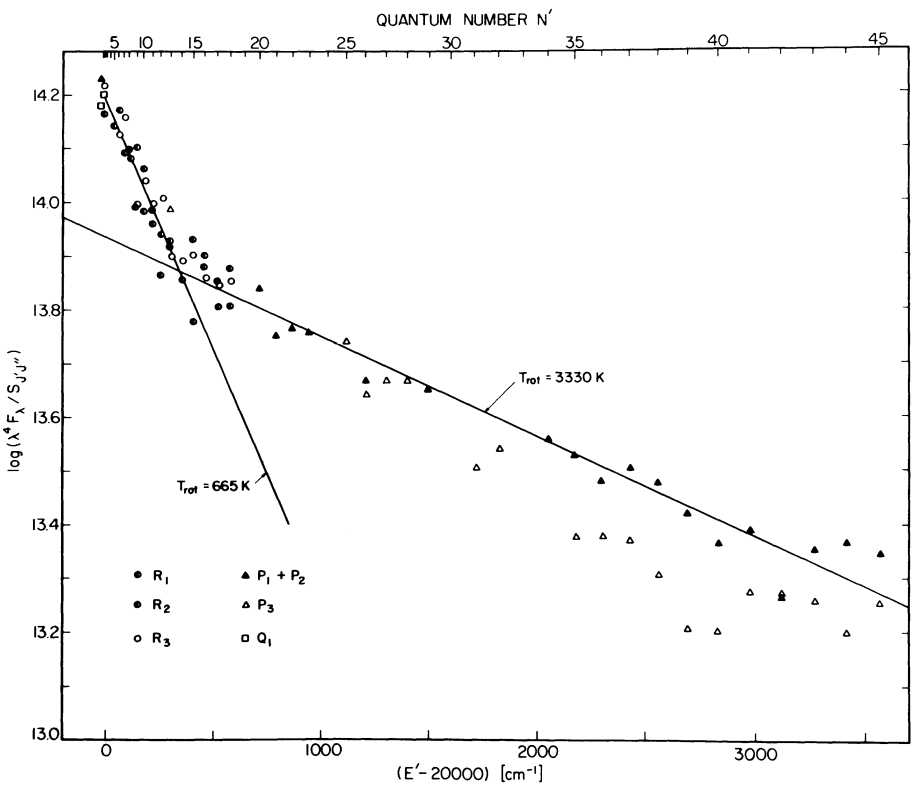

FIG. 4.—Rotational excitation of the C_2 $d\ ^3\Pi_g$ $v' = 0$ level in comet Halley. In this Boltzmann plot, a rotational temperature of 3330 K is seen to fit the high J' levels that provide the $P_1 + P_2$ blends. A low temperature, $T_{rot} = 665$ K, fits all of the low rotational levels.

© American Astronomical Society • Provided by the NASA Astrophysics Data System

1990ApJ...353..640L

TABLE 2

THE C_2 SWAN 0–0 LINES

λ_{air} (Å)	Line	E' (cm^{-1})	$S_{J'J''}$	F_λ	λ_{air} (Å)	Line	E' (cm^{-1})	$S_{J'J''}$	F_λ
5131.580	$P_1(47)$	23570	46.96	2.98	5147.107	$R_3(8)$	20184	8.89	1.39
5131.582	$P_2(46)$	23571	45.95		5147.682	$P_1(38)$	22299	37.95	3.22
5131.687	$P_3(45)$	23573	44.96	1.16	5147.682	$P_2(37)$	22300	36.94	
5132.350	$R_1(18)$	20581	18.86	2.04	5147.803	$P_3(36)$	22302	35.96	1.22
5132.488	$R_2(17)$	20584	17.85	1.65	5147.918	$R_1(9)$	20139	9.68	1.35
5132.690	$R_3(16)$	20596	16.93	1.74	5148.316	$R_2(8)$	20145	8.74	1.37
5133.704	$P_2(45)$	23417	44.95	3.05	5148.603	$R_3(7)$	20150	7.89	1.11
5133.706	$P_1(46)$	23415	45.96		5149.065	$P_1(37)$	22174	36.95	3.49
5133.812	$P_3(44)$	23417	43.96	1.00	5149.098	$P_2(36)$	22176	35.94	
5134.305	$R_1(17)$	20518	17.85	1.83	5149.201	$P_3(35)$	22177	34.96	1.19
5134.480	$R_2(16)$	20521	16.85	1.54	5149.323	$R_1(8)$	20107	8.63	1.54
5134.661	$R_3(15)$	20524	15.92	1.60	5149.775	$R_2(7)$	20114	7.71	1.32
5135.561	$P_1(45)$	23264	44.96	2.88	5150.547	$P_1(36)$	22053	35.95	3.64
5135.575	$P_2(44)$	23265	42.97		5150.547	$P_2(35)$	22055	34.94	
5135.685	$P_3(43)$	23267	42.97	1.12	5151.164	$R_2(6)$	20086	6.69	1.17
5136.261	$R_1(16)$	20458	16.84	1.82	5151.510	$R_3(5)$	20091	5.88	1.20
5136.432	$R_2(15)$	20462	15.84	1.84	5152.505	$R_2(5)$	20062	5.67	1.19
5136.651	$R_3(14)$	20465	14.92	1.55	5152.946	$R_3(4)$	20068	4.88	0.92
5137.573[a] ...	$P_2(43)$	23118	42.95	2.31	5153.287	$P_3(32)$	21825	31.96	1.56
5137.575[a] ...	$P_1(44)$	23116	43.96		5153.761	$R_2(4)$	20041	4.64	0.91
5137.683	$P_3(42)$	23118	41.97	1.12	5154.443	$P_3(31)$	21714	30.96	1.33
5138.100	$R_1(15)$	20402	15.83	1.93	5155.189	$R_1(3)$	19998	3.04	0.71
5138.306	$R_2(14)$	20406	14.83	1.27	5156.084[b] ...	$R_2(2)$	20010	2.55	0.81
5138.502	$R_3(13)$	20409	13.92	1.59	5156.130[b] ...	$R_1(2)$	19986	1.69	
5139.312	$P_1(43)$	22971	42.96	2.98	5156.523	$P_1(31)$	21499	30.94	3.85
5139.331	$P_2(42)$	22973	41.95		5156.572	$P_2(30)$	21501	29.93	
5139.439	$P_3(41)$	22974	40.97	1.10	5157.158	$R_2(1)$	20000	1.43	0.29
5140.133	$R_2(13)$	20354	13.81	1.42	5157.747	$P_3(28)$	21402	27.96	1.88
5140.372	$R_3(12)$	20357	12.91	1.44	5157.960[b] ...	$Q_1(5)$	20013	1.17	0.45
5141.194	$P_2(41)$	22832	40.95	2.98	5158.050[b] ...	$R_3(0)$	20009	0.96	0.30
5141.195	$P_1(42)$	22830	41.96		5158.180	$Q_1(4)$	19998	1.53	0.34
5141.310	$P_3(40)$	22833	39.97	0.91	5158.658	$P_3(27)$	21305	26.96	1.72
5141.637	$R_1(13)$	20301	13.79	1.63	5159.440	$P_1(28)$	21207	27.93	3.58
5141.886	$R_2(12)$	20305	12.80	1.55	5159.466	$P_2(27)$	21209	26.93	
5142.107	$R_3(11)$	20309	11.91	1.35	5159.592	$P_3(26)$	21211	25.96	1.60
5142.817	$P_1(41)$	22692	40.95	3.18	5160.377	$P_3(25)$	21121	24.95	1.92
5142.839	$P_2(40)$	22694	39.95		5160.565[b] ...	$P_2(2)$	19994	1.46	0.55
5142.942[a] ...	$P_3(39)$	22695	38.97	0.90	5160.713[b] ...	$P_1(3)$	19977	1.71	0.45
5143.323[a] ...	$R_1(12)$	20255	12.77	1.33	5161.022[b] ...	$P_1(26)$	21030	25.92	5.57
5143.589	$R_2(11)$	20260	11.79	1.46	5161.045[b] ...	$P_2(25)$	21032	24.92	
5143.856	$R_3(10)$	20264	10.90	1.58	5161.367[b] ...	$P_1(4)$	19986	3.07	0.73
5144.564	$P_1(40)$	22558	39.95	3.37	5161.667	$P_1(25)$	20946	24.92	3.92
5144.564	$P_2(39)$	22559	38.94		5161.730	$P_2(24)$	20948	23.91	
5144.681	$P_3(38)$	22560	37.96	1.10	5162.339	$P_1(24)$	20866	23.91	3.82
5144.913	$R_1(11)$	20213	11.75	1.62	5162.373	$P_2(23)$	20869	22.91	
5145.224	$R_2(10)$	20218	10.77	1.40	5162.862	$P_1(23)$	20790	22.91	3.53
5145.470	$R_3(9)$	20222	9.90	1.40	5162.929	$P_2(22)$	20792	21.91	
5146.065	$P_1(39)$	22427	38.95	3.51	5163.396[b] ...	$P_1(22)$	20717	21.90	4.15
5146.097	$P_2(38)$	22428	37.94		5163.435[b] ...	$P_2(21)$	20719	20.91	
5146.199	$P_3(37)$	22430	36.96	1.24	5165.221[b] ...	$P_3(14)$	20357	13.94	5.28
5146.460	$R_1(10)$	20174	10.72	1.76	5165.241[b] ...	$P_3(13)$	20309	12.94	
5146.802	$R_2(9)$	20180	9.76	1.34	5165.246[b] ...	$P_3(12)$	20264	11.94	

[a] Not plotted in Fig. 4. Line appears too weak: coincides with a Fraunhofer line.
[b] Not plotted Fig. 4. Line appears too strong: known or suspected blend.

Estimates of the relative populations in the F_1 and F_2 levels contributing to an unresolved $P_1 + P_2$ blend are obtained from the observed wavelengths of the blends. Thanks to the Λ-type doubling and the absence of the antisymmetric levels, the P_1 and P_2 lines may be effectively coincident when N'' is odd ($J'' = N''$ for F_2) but slightly separated when N'' is even. For example, Amiot (1983) assigns P_1 and P_2 an identical wavelength for $N'' = 37$, but P_2 is displaced 32 mÅ to the red of P_1 for $N'' = 38$; at our dispersion, the 32 mÅ displacement is equivalent to about 1.5 diodes. The uncertainty of these laboratory measurements appears to be a few mÅ. An imbalance of the population of F_1 relative to F_2 will cause the measured wavelengths of the even-N'' $P_1 + P_2$ blends to shift relative to the odd-N'' blends. The wavelengths of all unblended $P_1 + P_2$ blends were measured with respect to the radial velocity determined by the many unblended R-branch lines across the bandpass. Our technique was tested against the spectrum of the acetylene flame where it is expected that the F_1 and F_2 level should be equally populated; the measured wavelength shifts $\delta\lambda$ are shown in Figure 5*a* where the odd-N'' and even-N'' blends are seen to give the same small shifts with a hint of a N'' dependence. Results from our highest S/N nightly average of cometary spectra (Mar 29) are shown in Figures 5*b* and 5*c*; the wavelength shifts necessary to achieve the co-addition of

© American Astronomical Society • Provided by the NASA Astrophysics Data System

1990ApJ...353..640L

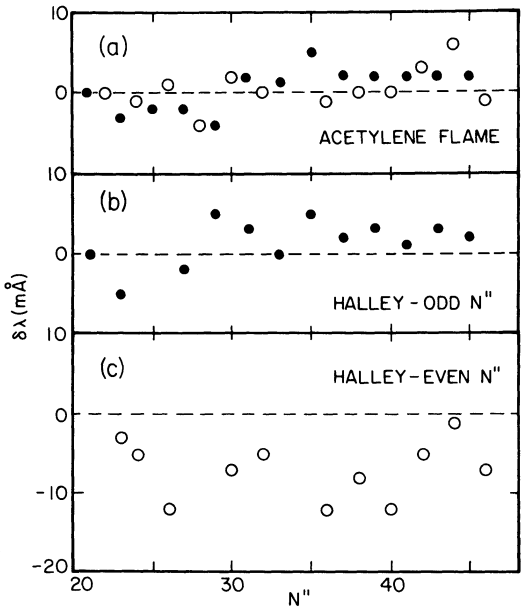

FIG. 5.—Wavelength shifts of the $P_1 + P_2$ blends relative to a scale defined by unblended R-branch lines. In panel (*a*), the measured shifts for the acetylene flame show no odd-even N'' effect. Such an odd-even effect is clearly seen for comet Halley—see panels (*b*) and (*c*).

spectra from two or more nights necessarily compromise a search for such small wavelength shifts. Comparison of Figure 5*b* and 5*c* clearly shows that the even-N'' blends are systematically displaced relative to the odd-N'' blends. The differential shifts between acetylene flame and the comet should remove small errors in the adopted laboratory wavelengths and systematic shifts over the bandpass introduced by the spectrometer. The even-N'' blends for $N'' \gtrsim 26$ are clearly displaced (Fig. 6) such that the F_1 levels at a given N'' are from 2 to 4 times more populated than the F_2 levels. For $N'' \lesssim 24$, the F_1 and F_2 levels appear more equally populated. For $N'' \gtrsim 40$, the P_1 and P_2 lines of odd N'' are moving into coincidence, and the mean wavelength is insensitive to the relative populations of F_1 and F_2. At $N \simeq 20$, the even-N'' and odd-N'' blends show similar wavelength displacements between the P_1 and P_2 components of a blend.

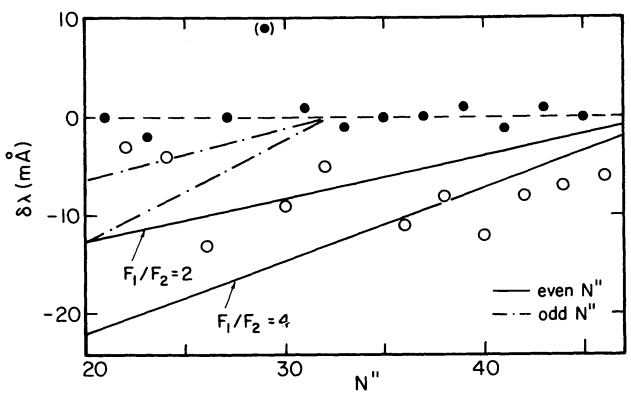

FIG. 6.—Wavelength shifts of the $P_1 + P_2$ blends in comet Halley relative to the acetylene flame. The even N'' for $N \geq 30$ blends are displaced in the comet's spectrum, suggesting that the F_1 level is overpopulated relative to the F_2 level. Predicted shifts are shown for odd and even N'' for population ratios of $F_1/F_2 = 2$ and 4.

If our observations refer to a single sample of fluorescing molecules, the derived T_{rot}'s describe correctly the change in population between the low and the high rotational levels. However, two or more quite distinct samples of C_2 molecules may have contributed to the spectra. Since the rotational excitation of molecules freshly created from parent molecules probably differs from that of the relaxed fluorescing C_2 molecules, the concept of more than a single sample of molecules merits attention. If a sample of rotationally cold and a second sample of rotationally hot molecules have produced the observed spectrum, the contribution of the 3000 K component to the fluxes of the low-J lines should be subtracted prior to a calculation of T_{rot} for the low-J levels. When the fluxes are corrected for the 3000 K component, the low-J lines give an even lower rotational temperature: $T_{rot} = 190 \pm 25$ K. These corrections are based on an assumption that the populations of the low-J levels in the hot component are described by the rotational temperature derived of the high-J' levels; predictions (see below) indicate that this assumption is invalid. Since the T_{rot} for the high-J levels is determined from lines spanning a larger range in excitation energy, the influence of the low T_{rot} on the high T_{rot} is much smaller than the reverse dependence. The rotationally cold molecules are in the minority: $n(190)/n(3330) \simeq 0.05$ for $v' = 0$, where n is the number of molecules in all rotational states. If it is assumed that the rotationally cold molecules have a low vibrational temperature and the rotationally hot molecules have a vibrational temperature similar to that predicted by Gredel, van Dishoeck, and Black (1989, hereafter GvDB), the ratio is reduced to $n(190)/n(3330) \simeq 0.02$.

A skeptic may assert that the low rotational temperature is merely a reflection of a systematic error affecting the measurements of the fluxes of the low-J' and, hence, weakest lines in the sample. There are three strong reasons for dismissing such an assertion: (1) the lines in question are well defined; (2) an identical treatment of the spectrum of the acetylene flame does not yield a low rotational temperature; and (3) a similar low rotational temperature was found for comet West 1976 VI using a different spectrometer. Points (2) and (3) are discussed below. Inspection of Figures 1, 2, and 3 shows that a majority of the lines with $J' < 15$ that define the cold low-J populations are well resolved from neighboring lines and have a peak intensity that is many times the noise level. Since the scatter of the points about the $T_{rot} = 665$ K line in Figure 4 is small, the random errors of measurement are assuredly unimportant. As noted above, the individual spectra consistently show a low rotational temperature for the low-J' levels. To within the errors of measurement, the derived T_{rot}'s are almost identical and independent of the signal-to-noise ratio of the spectra.

As a partial check on the integrity of the observational techniques and reductions, we analyzed the spectra of the acetylene flame: a single temperature, $T_{rot} = 2980 \pm 25$ K, provides a good fit to these lines (Fig. 7). Of special note is the equivalence of the $P_1 + P_2$ blends and the P_3 lines in Figure 7. This result, which is consistent with independent analyses of C_2 Swan bands from acetylene flames (LD), strongly suggests that the striking imbalance seen in comet Halley between $P_1 + P_2$ and P_3 is not due to a systematic error afflicting the measured fluxes. Furthermore, the absence from the flame's C_2 molecules of a low T_{rot} sample at the beginning of the rotational ladder again suggests that the evidence (Fig. 4) for such a sample in comet Halley is valid.

Independent evidence for the low T_{rot} was provided earlier by high-resolution scans of short-wavelength intervals at

© American Astronomical Society • Provided by the NASA Astrophysics Data System

1990ApJ...353..640L

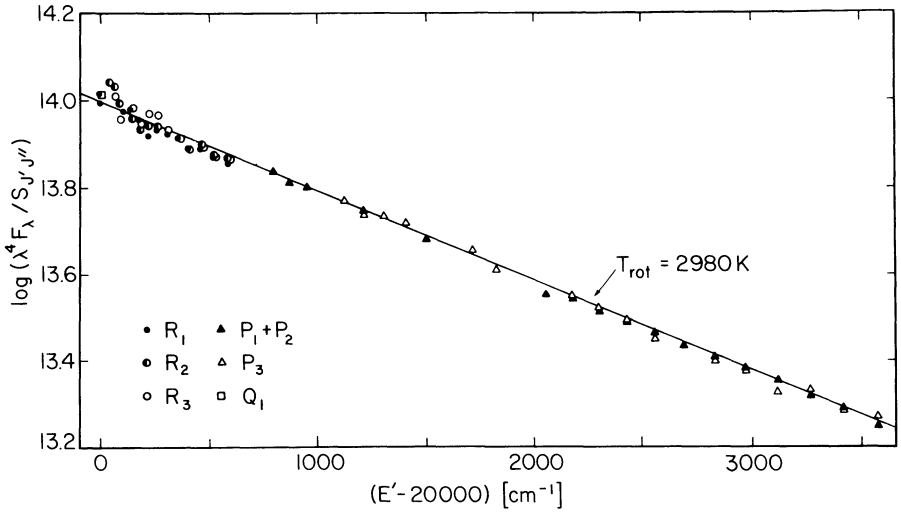

FIG. 7.—Rotational excitation of the C_2 $d\ ^3\Pi_g$ $v' = 0$ level in an acetylene flame. In this Boltzmann plot, a rotational temperature $T_{rot} = 2980$ K is seen to describe the population except for a few aberrant points (blends?) among the initial levels of the rotational ladder.

several wavelengths across the 0–0 Swan band emitted by comet West 1976 VI (LD). A comparison of the integrated flux of a *P*-branch triplet with the flux of the adjacent *R*-branch triplet to the red gave a T_{rot} in the range 3000–3500 K. For the lines involved in the comparisons of *P* and *R* branch, we predict from Figure 4 $T_{rot} \sim 3200$ K, a value in good agreement with the values obtained for comet West. At the resolution employed by LD, the P_3 line was generally not resolved from the close blend of P_1 and P_2. In the two cases where the necessary resolution was achieved, the *P* triplet was blended with low-*J* branch lines so that the spectra cannot be used to check that the P_3 levels are underpopulated relative to F_1 and F_2. A scan near 5160 Å enabled LD to measure the flux ratio of $P_2(2)$ and $P_1(3)$ to $P_3(25)$ and to obtain "the low excitation temperature of 1400 K." Other scans near the 0–0 band's origin prompted the comment "These low *P* lines and also the *Q* branch lines suggest that the lowest rotational levels in $v'' = 0$ are overpopulated relative to the higher levels." Our present spectra fully confirm this earlier observation; the relation portrayed in Figure 4 suggests $T_{rot} \sim 1500$ K for the excitation temperature of the levels that provided LD's low *P* and *Q* and the high *P* lines. It is apparent that LD's spectra anticipated the results presented here. The confirmation of our results is significant because the two series of observations were obtained with different spectrometers and observing and reduction techniques, and, hence, it is most unlikely that systematic errors are responsible for the interesting population distribution shown in Figure 4.

In the sequence of spectra taken in 1986 April at different positions with respect to the nucleus, the ratio of "cold" to "hot" molecules varies slightly with position. Although these spectra were obtained at a lower resolution than the spectra just discussed, an adequate number of C_2 lines and blends are available for a determination of the relative number of "cold" and "hot" molecules. Our summed spectrum from 1986 March was degraded to the lower resolution of the later observations and the C_2 features remeasured off the 1986 March spectrum. The on-nucleus spectrum from 1986 April differs slightly from the mean spectrum for 1986 March. From Figure 8 where the fluxes for the high-*J'* features have been made coincident, the "cold" molecules are clearly seen to be about

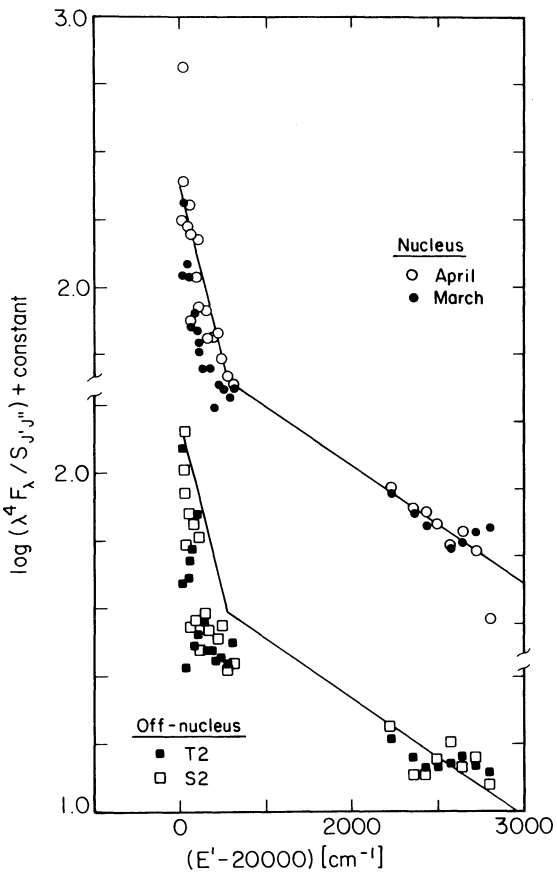

FIG. 8.—Rotational excitation of the C_2 $d\ ^3\Pi_g$ $v' = 0$ level in comet Halley. Boltzmann plots are compared at the top for observations from March and April in which the spectrometer's entrance slit was approximately centered on the nucleus; the solid line in two segments is a fit to the April data. Similar plots are shown at the bottom for observations taken in April with the entrance slit centered about 40″ from the nucleus; the solid line fitted to the April (nucleus) data is here shifted to fit the high-*J'* data from these off-nucleus spectra.

© American Astronomical Society • Provided by the NASA Astrophysics Data System

1990ApJ...353..640L

twice as abundant in April than March. This change may be associated with the increase in the comet's heliocentric from about 1.1 AU in late March to 1.3 AU in early April. Examination of the March spectra shows that daily changes of up to $\pm 25\%$ in the ratio of "cold" to "hot" populations occurred.

A pronounced variation in this ratio occurs across the face of the comet. Figure 8 shows that the rotational populations are very similar at 40″ from the nucleus toward (S2) and away (T2) from the Sun; the same conclusion holds for the spectra taken at 20″ from the nucleus. The "cold" molecules are relatively less abundant at 40″ from the nucleus, and their temperature has dropped. When the rotational temperature is derived from the low-J' lines without a correction for a sample at the higher T_{rot} suggested by the high-J' features, the nuclear spectrum gives $T_{rot} \simeq 500$ K, and the spectra taken at 40″ from the nucleus give $T_{rot} \sim 300$–400 K. The T_{rot} derived from the few high-J' features appears to increase away from the nucleus: $T_{rot} = 2540 \pm 200$ K on the nucleus, 3300 ± 200 K at 20″, and 4110 ± 310 K at 40″ from the nucleus. These systematic variations of the ratio of "cold" to "hot" molecules and their T_{rot}'s with position are a challenge to the view that the C_2 emission is dominated by simple fluorescence of C_2 molecules in sunlight in an optically thin environment. The variations imply that care must be taken in acquiring and interpreting observations intended to measure the heliocentric dependence of line and band ratios.

In principle, clues to the origins of the variation of rotational temperature with excitation energy may be found in a similar analysis of a Phillips ($A\ ^1\Pi_u$–$X\ ^1\Sigma_g^+$) band. Appenzeller and Münch (1987, hereafter AM) derive a high rotational temperature ($T_{rot} \simeq 10{,}300$ K) from a high-resolution CCD spectrum of the Phillips 2–0 band taken on 1986 March 5. Our reanalysis of AM's observations suggests that a lower T_{rot} may provide an acceptable fit. AM give the measured peak intensities (I_λ) from a 2″ by 8″ region centered 11″ west of the nucleus. When the selection of lines is restricted to those of highest quality (no blending C_2 or airglow OH lines, etc.), a rotational temperature $T_{rot} \simeq 3000$ K provides an adequate fit to all but two lines. AM's high rotational temperature results when three high-J R lines are given great weight, but two of this trio are not of the highest quality. A conservative view is that AM's data admits a considerable range in the rotational temperature for the $v' = 2$ level of the $A\ ^1\Pi_u$ state. There is no evidence for a low rotational temperature for the initial levels of the rotational ladder for $v' = 2$ level of the $A\ ^1\Pi_u$ state, but before one can claim with confidence that "cold" molecules are detected through the Swan bands but not the Phillips system, additional observations of the Phillips (and other singlet) system in comets are desirable.

IV. ROTATIONAL EXCITATION OF C_2

a) *Predicted Populations and Spectra*

At the low densities prevailing in comets, collisional processes are generally supposed not to contribute to the molecule's statistical equilibrium. Since the time required to establish this statistical equilibrium is short relative to the lifetime of the molecule, it is supposed that the rates of formation from a parent molecule and of destruction through photodissociation (or photoionization) may be omitted from the equations describing statistical equilibrium of a molecule.

Studies of the statistical equilibrium of C_2 and of the excitation of the Swan bands have generally considered the vibrational excitation of the electronic states but ignored the rotational structure of the states. The most ambitious study of the vibrational populations is by Krishna Swamy and O'Dell (1987) who adopt a model molecule with 14 vibrational levels for each of five singlet and five triplet electronic states. For the C_2 Swan bands, the processes contributing to the statistical equilibrium of the upper ($d\ ^3\Pi_g$) state include transitions within the Swan system ($d\ ^3\Pi_g$–$a\ ^3\Pi_u$) and the Ballik-Ramsay system ($b\ ^3\Sigma_g$–$a\ ^3\Pi_u$), and the intercombination transition $a\ ^3\Pi_u$–$X\ ^1\Sigma_g^+$. Since the vibrational ladders of the $a\ ^3\Pi_u$ and $X\ ^1\Sigma_g^+$ states overlap, intercombination transitions $a\ ^3\Pi_u \rightarrow X\ ^1\Sigma_g^+$ may depopulate the former by spontaneous emission as it is repopulated by spontaneous emissions from $X\ ^1\Sigma_g^+$ vibrational levels lying above $a\ ^3\Pi_u$ states. Of course, the intercombination transition is too weak to introduce significant upward excitation of the vibrational ladders by absorption of sunlight. Krishna Swamy and O'Dell (1979, 1981) were the first to recognize that the a–X intercombination transitions are effective in controlling the relative equilibrium populations of the lowest singlet and triplet states as well as their relative vibrational populations (i.e., their vibrational temperatures). As first shown by Krishna Swamy and O'Dell (1977), the principal effect of the Ballik-Ramsay system on the equilibrium population of $a\ ^3\Pi_u$ and, hence, on $d\ ^3\Pi_g$ and the Swan bands, arises because the higher ($v \geq 4$) vibrational levels of $a\ ^3\Pi_u$ may decay by spontaneous emission to lower vibrational levels via $b\ ^3\Sigma_g^-$, e.g., $a\ ^3\Pi_u\ (v \geq 4) \rightarrow b\ ^3\Sigma_g^-\ (v') \rightarrow a\ ^3\Pi_u\ (v'')$. This chain reduces the vibrational temperature of the low vibrational levels of $a\ ^3\Pi_u$. The electric dipole vibration-rotation transitions that cool vibrational ladders for heteronuclear diatomic molecules are forbidden for homonuclear molecules like C_2; the electric quadrupole vibration-rotation transitions are too weak to affect the rotational equilibrium. Radiative excitation via the Ballik-Ramsay system is a minor contributor to the statistical equilibrium; the system has a small f-value, and the flux of infrared solar photons is low.

A prediction of the level populations in statistical equilibrium calls for a suite of molecular data (energy levels, and Einstein A-values or their equivalent such as the electronic transition moments $|R_e|^2$, expressed in atomic units [au]). For C_2, accurate data are available for most of the transitions controlling the emission of the Swan bands except, perhaps, for the intercombination transitions. Exploratory calculations (Krishna Swamy and O'Dell 1987) suggest that a–X is the dominant intercombination transition, and, therefore, $|R_e|^2_{aX}$ becomes the leading ("molecular") uncertainty affecting predictions of the Swan band intensities.

Since the predicted relative intensities of the Swan bands are dependent on $|R_e|^2_{aX}$, observations of the band fluxes can provide an estimate of this electronic transition moment. A majority of observations refer to the ratio of the fluxes in the sequences $\Delta v = 0$ (i.e., 0–0, 1–1, ...) with its origin at 5165 Å to $\Delta v = +1$ (i.e., 1–0, 2–1, ...) with its origin at 4737 Å. O'Dell *et al.* (1988) provide new measurements of the flux ratio $R = F(\Delta v = +1)/F(\Delta v = 0)$ for comet Halley over heliocentric distances $0.9 < r(\mathrm{AU}) < 2.2$. These results are extracted from long-slit CCD spectra from five nights from 1985 October to 1986 May. O'Dell *et al.* (1988), who provide references to the numerous, earlier attempts to measure this ratio in Halley and other comets, argue that their new results provide the most accurate data to date. Long-slit CCD spectra (Beisser *et al.* 1989) of comet P/Tempel 2 at $r = 1.5$ AU confirm the values of R found by O'Dell *et al.* for comet P/Halley. Comparison of

© American Astronomical Society • Provided by the NASA Astrophysics Data System

1990ApJ...353..640L

the observed and predicted ratios R (Krishna Swamy and O'Dell 1987) led O'Dell *et al.* to obtain $|R_e|^2_{aX} = 2.5 \times 10^{-6}$.

Our determinations of the rotational excitation temperature for $v = 0$ level of the $d\ ^3\Pi_g$ state will be interpreted in light of the extensive study of the vibration-rotation excitation of cometary C_2 molecules by GvDB. The model molecule (Fig. 9) consisted of six electronic states. For each state, the vibrational levels $v = 0$–5 and the 60 lowest rotational levels of each vibrational level were included. All significant routes involving excitation by absorption of solar photons and deexcitation by spontaneous and stimulated emission were included in the equations of statistical equilibrium. The level populations in equilibrium are, of course, dependent on the adopted electric dipole transition moments for the transitions A–X (the Phillips system), d–a (the Swan system), b–a (the Ballik-Ramsay system), and d-c (an as yet unobserved transition).

Two intercombination transitions a–X and c–X were considered. Since the a–X, and to a lesser extent the c–X, intercombination transitions can influence $T_{\rm rot}$, we discuss in some detail GvDB's various representations of the electric transition moments $|R_e|^2_{aX}$ and $|R_e|^2_{cX}$. The transition probability for spontaneous emission was calculated from the expression

$$A_{v'J',\,v''J''} = \frac{64\pi^4}{3h}\,\sigma^3\,\frac{\sum_N |R_e|^2}{N}\,q_{v'v''}\,\frac{S_{J'J''}}{2J'+1}\,,$$

where $q_{v'v''}$ is the Franck-Condon factor, $S_{J'J''}$ is the Hönl-London factor (rotational line intensity), and N is the number of independent transition moments ($N = 1$ for c–X, $N = 2$ for a–X). The reader is referred to GvDB for detailed discussions of the factors $|R_e|^2$, $q_{v'v''}$, and $S_{J'J''}$.

The magnitude of $|R_e|^2$ for the intercombination transitions is controlled by the spin-orbit interaction that causes a mixing of singlet and triplet states; for example, the principal mixings influencing the a–X transition are between $a\ ^3\Pi_u$ and $A\ ^1\Pi_u$ and between $X\ ^1\Sigma_g^+$ and $b\ ^3\Sigma_g^-$. Three different schemes for estimating the transition moments $|R_e|^2$ of the intercombination transitions are described by GvDB:

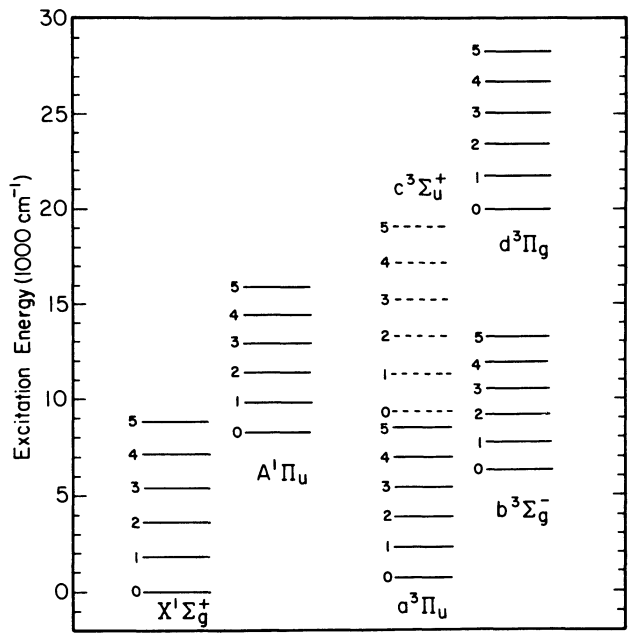

FIG. 9.—C_2 term diagram showing the lowest electronic states (after Gredel *et al.* 1989).

1. The $|R_e|^2$ were estimated from fits of synthetic spectra to a spectrum of the Swan (0, 0) band obtained in 1985 December at a resolution $\lambda/\Delta\lambda \approx 24{,}000$. When $|R_e|^2$ is assumed to be independent of vibration and rotation, $|R_e|^2_{aX} \approx 3.5 \times 10^{-6}$ and $|R_e|^2_{cX} \approx 3.5 \times 10^{-6}$ to 2×10^{-5} are derived. The value for $|R_e|^2_{aX}$ is similar to the value (2.5×10^{-6}) estimated by O'Dell *et al.* (1988) from the variation of the band ratio R with heliocentric distance. O'Dell *et al.* adopt a model C_2 molecule in which rotational structure is suppressed. GvDB's calculations include an insufficient number of vibrational levels to permit an accurate prediction of R when R is taken to refer to the entire $\Delta v = 0$ and -1 sequences. A direct comparison of O'Dell *et al.*'s low-resolution spectra and GvDB's synthetic spectra would be of great interest.

2. GvDB estimate the transition moments $|R_e|^2$ using spin-orbit matrix elements from an unpublished calculation by R. Klotz. The end product of GvDB's procedure is an estimate for $|R_e|^2$ for the vibrational bands (v', v'') of the a–X and the c–X transitions. These estimates depend on the $|R_e|^2$'s for the permitted transitions. Since the $|R_e|^2$ for the Swan system is well determined from lifetime measurements and the $|R_e|^2$ for the Ballik-Ramsay system is only a weak contributor to the $|R_e|^2$ of the intercombination transitions, the $|R_e|^2$ for Phillips system is the leading source of uncertainty: lifetime measurements for the $A\ ^1\Pi_u$ state (Bauer *et al.* 1985, 1986) yield a $|R_e|^2$ that differs by almost a factor of 2 from the series of fairly concordant theoretical predictions (see summary by O'Neil, Rosmus, and Werner 1987). This uncertainty translates to about a 50% uncertainty in $|R_e|^2_{aX}$ but a larger uncertainly in $|R_e|^2_{cX}$. Estimates of $|R_e|^2_{aX}$ by this method are smaller than the estimates obtained from fits of synthetic and observed spectra, and the band ratio R. Estimates of $|R_e|^2_{cX}$ overlap the range suggested by the fit to the observed spectra. GvDB point out that, because of the rotational dependence, such estimates of $|R_e|^2$ are "likely to be lower limits to the effective intercombination transition moments that determine the rotational transition probabilities."

3. The spin-orbit interaction has a rotational dependence that is ignored when the transition moment is taken to be a product of a (fixed) $|R_e|^2$, a Franck-Condon factor $q_{v'v''}$, and a Hönl-London factor $S_{J'J''}$. A theoretical calculation of the rotational dependence ($J \leq 30$) for the a–X transition was reported by Le Bourlot and Roueff (1986); GvDB, who note some limitations of this study, report on fluorescence calculations in which transition probabilities for the a–X transition are taken from Le Bourlot and Roueff (1986) for $J \leq 30$ and extended to higher J values using a rotationally independent $|R_e|^2$ (see § I).

GvDB give an extensive discussion of the dependence of the equilibrium populations of the $A\ ^1\Pi_u$ and $d\ ^3\Pi_g$ states on the principal variables (e.g., the comet's heliocentric distance) and the leading sources of uncertainty (e.g., the transition moments for the A–X, a–X, and c–X transitions). GvDB use the observed solar flux spectrum so that the effects of the Fraunhofer lines on the rate of radiative excitation for specific transitions are included.

The surface brightness distribution of the C_2 Swan bands over the comet's coma was analyzed by O'Dell *et al.* (1988) who concluded that the C_2 molecule is a third-generation molecule; i.e.,

$$\mathrm{Y} \rightarrow \mathrm{Z} + L$$
$$\mathrm{Z} \rightarrow \mathrm{C_2} + M$$
$$\mathrm{C_2} \rightarrow \mathrm{C} + \mathrm{C}\,,$$

© American Astronomical Society • Provided by the NASA Astrophysics Data System

1990ApJ...353..640L

where L and M are atomic or molecular fragments and the molecules Y (grandparent), Z (parent of C_2), and C_2 are considered to be photodissociated by the sunlight. Possible identifications are $Y \equiv C_2H_2$ and $Z \equiv C_2H$. The products from photodissociated C_2 are not necessarily limited to two neutral C atoms. Analysis of the surface brightness distribution in terms of Haser's (1957) model gave the scale lengths for the density (n) gradient of a molecule ABC destroyed through photodissociation: $n(\mathrm{ABC}) \propto \exp(-r/r_{\mathrm{ABC}})$, where r is the distance from the comet's nucleus: O'Dell *et al.* obtained $r_Y \sim 15{,}000$ km, $r_Z \sim 7500$ km, and $r_{C_2} \sim 75{,}000$ km. During our observations in 1986 March, these scale lengths corresponded to angular sizes of $\theta_Y \sim 20''$–$40''$, $\theta_Z \sim 10''$–$20''$, $\theta_{C_2} \sim 100''$–$200''$. Statistical equilibrium is achieved for C_2 in about 500 s (LD; O'Dell *et al.* 1988). Since gas in the coma of a comet at the observed heliocentric distance expands outward at a velocity of about 1 km s^{-1}, equilibrium is achieved within about 500 km of the site of the formation of the C_2 molecule. Formation of C_2 molecules occurs over a range of distances from the nucleus that is roughly equal to $r_Y + r_Z$ and, hence, to angular distances of $30''$–$50''$ for our observations; i.e., freshly formed C_2 molecules contributed to our recorded spectrum. In April when our lower resolution spectra were obtained on and off the nucleus, the comet was closer to earth, and the maximum angular separation of $40''$ corresponds to about 13,000 km, and even this line of sight must contain some freshly formed C_2 molecules whose rotational populations may differ from the equilibrium values achieved through fluorescence.

b) Observed and Predicted Populations for d $^3\Pi_g$

Through a comparison of synthetic and observed spectra, GvDB estimated that $|R_e|^2_{aX} \simeq 3.5 \times 10^{-6}$ and $|R_e|^2_{cX} \approx 3.5 \times 10^{-6}$ or 2×10^{-5} au for $A_{dc}/A_{da} = 0.1$ or 0.03, respectively, when a theoretical estimate (van Dishoeck 1983) is adopted for the transition moment of the Phillips system. Predicted populations for $d\ ^3\Pi_g$ ($v = 0$) are shown in Figure 10 for $|R_e|^2_{aX} = |R_e|^2_{cX} = 3.5 \times 10^{-6}$, a heliocentric distance of 1.1 AU and a heliocentric radial velocity of -27 km s^{-1}. Populations for the $^3\Pi_0$, $^3\Pi_1$, and $^3\Pi_2$ substates are shown separately. The distance and velocity were the appropriate values for comet Halley in 1985 December when the spectra considered by GvDB were obtained. Our high-resolution spectra were obtained in 1986 March when the comet was at a distance of 0.85–1.15 AU with a heliocentric radial velocity of +24.9–26.8 km s^{-1}. The heliocentric distance, but not the radial velocity, for our observations is close to GvDB's assumed values.

Notable features of these predictions are testable using our observations:

1. The striking differences in the populations of the three substates at low J' (≤ 15). Note especially that the populations of first few rotational levels of $^3\Pi_2$ are a factor of 4 smaller than for the same J values in $^3\Pi_1$.

2. Differences between the substates persist for the higher rotational levels ($J' \geq 15$) but are smaller. For the J' interval covered by our observations, the predicted T_{rot} are approximately 3300 K ($^3\Pi_0$), 3000 K ($^3\Pi_1$), and 4300 K ($^3\Pi_2$).

3. There is a pronounced odd-even variation of the populations.

4. The odd-even variation is randomly distorted; strong Fraunhofer lines reduce the excitation rate to particular levels. Since there is a difference of about 50 km s^{-1} between the radial velocity adopted for the predictions and the value appropriate to our observations, we should not expect the small and irregular level-to-level predicted differences of populations to be reproduced in our observations.

Since the transition moments corresponding to the predictions provide a synthetic spectrum that apparently closely matched observed spectra available to GvDB, one expects the predicted populations to match those derived from our spectra. Even a cursory comparison of Figures 4 and 10 shows that the first of the above predictions is not confirmed by our spectra. As we have argued above, the principal characteristics of the C_2 population as revealed by Figure 4 are most unlikely to be distorted by systematic errors. In particular, the low T_{rot} at low J' that is so obvious from Figure 4 was revealed earlier in comet West with observations taken with a different spectrometer and detector. We suspect that detailed scrutiny of GvDB's observed spectra would reveal an overpopulation of the low-J' levels. We further comment below on the observed populations for $J' \leq 15$.

Since for $J' \geq 20$, $^3\Pi_1$, and $^3\Pi_2$ are not sampled individually, we have constructed from the predicted populations an equivalent plot (Figure 11) to Figure 4 where the $P_1 + P_2$ blends and P_3 lines constitute the observations for $J' \geq 20$. Comparison of Figures 4 and 11 show that the predictions account for the observations at $J' \gtrsim 15$ quite well. The observed variation of the populations (i.e., T_{rot}) across the

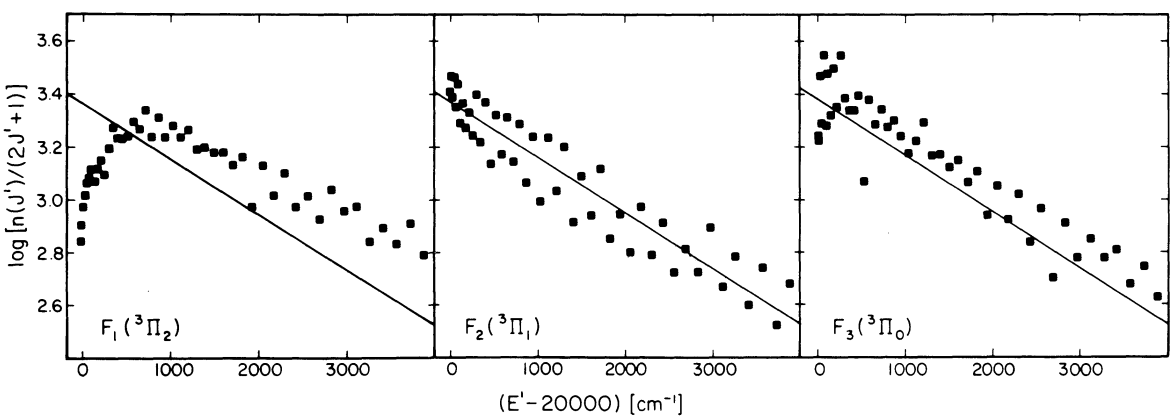

FIG. 10.—Predicted rotational population of the C_2 $d\ ^3\Pi_g$ $v' = 0$ levels for the conditions described in the text. The straight line in each panel corresponds to $T_{\mathrm{rot}} = 3000$ K and is a fair description of the populations in F_2 ($^3\Pi_1$).

© American Astronomical Society • Provided by the NASA Astrophysics Data System

1990ApJ...353..640L

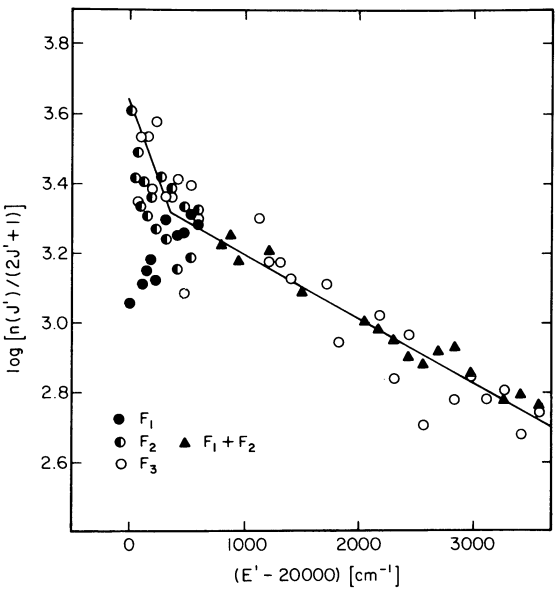

FIG. 11.—Predicted rotational excitation of the C_2 $d\ ^3\Pi_g$ $v' = 0$ level. Compare this figure and Fig. 4. The solid line is taken from the fit to the observations in Fig. 4. Predictions are given here for the levels and combinations of levels represented by the observations.

observed range is predicted to be within the observational and theoretical uncertainties. The observed lower T_{rot} associated with the P_3 lines is predicted. Close scrutiny of the observed wavelengths of the $P_1 + P_2$ blends shows, as described above, that $^3\Pi_2$ (F_1) and $^3\Pi_1$ (F_2) levels are unequally populated. The predictions reproduce the sense of this inequality. Since the observational estimate, $n(F_1)/n(F_2) \sim 3$ depends on the measurement and analysis of small (subdiode) wavelength shifts, the smaller predicted ratio of $n(F_1)/n(F_2) \simeq 1.3$ may be considered to be consistent with the observations. Even closer agreement between observation and prediction for $J' \gtrsim 15$ would seem to be possible by adjustment of the key transition moments—see GvDB for a discussion.

Agreement between the observed and predicted populations does not extend to the low-J' levels. In particular, the observations show that the levels of the $^3\Pi_0$, $^3\Pi_1$, and $^3\Pi_2$ substates define a single relation in Figure 4, but the predictions give different relations (Fig. 10). When the predictions for the observed levels are examined (Fig. 11), it is seen that the observed and predicted populations at low J' are in fair agreement for F_2 and F_3, but the predicted populations of F_1 at low J' differ strikingly from the observed values. This striking discrepancy at low J' led us to discuss three questions:

1. Can an acceptable fit of the predictions to the observations be found by retaining the model C_2 molecule and adjusting the transition moments of the intercombination transitions within reasonable bounds?

2. Does GvDB's (1989) study of C_2 molecules fluorescing in sunlight overlook processes that have a controlling influence on the statistical equilibrium of the low-J levels?

3. Is there a significant contribution to the observed spectrum from molecules that are not fluorescing in equilibrium? In particular, what is the contribution from C_2 molecules in the interval between their formation by photodissociation from a parent molecule and the attainment of equilibrium with the sunlight?

Our summary of the procedures employed to estimate the transition moments $|R_e|^2_{aX}$ and $|R_e|^2_{cX}$ suggests that one explore first whether the observations and predictions for $J' \lesssim 15$ may be reconciled by selecting different values of these (or other) transition moments. We can partially explore this possibility thanks to R. Gredel who kindly made available predictions of $d\ ^3\Pi_g$ populations for a variety of assumed transition moments. These predictions refer to cases in which $|R_e|^2_{aX}$ and $|R_e|^2_{cX}$ are assumed to be independent of vibration and rotation. As illustrated by Figure 11, the observations and predictions for F_2 and F_3 at low (and high) J' are in fair agreement, but there is a striking discrepancy between observation and prediction for F_1. Although the change of slope from high J' to low J' is predicted for our selection of F_2 and F_3 lines, the scatter of the predictions at low J' about a mean trend is noticeably larger than the observed scatter. The discrepant slope for F_1 at low J' persists as $|R_e|^2_{aX}$ and $|R_e|^2_{cX}$ are varied widely. Although the predictions available to us do not allow us to investigate whether an improved fit to the observations at low J' is achieved when the transition probabilities for the a–X system are taken from Le Bourlot and Roueff (1986), we suspect that the observed and predicted populations at low J' cannot be reconciled by reasonable adjustments of the transition moments.

In examining potential answers to the second of the three questions, we considered the model C_2 molecule and searched for an overlooked radiative process that is unselective with respect to the F_1, F_2, and F_3 substates and that is faster at low J values than the intercombination transitions. Our examination of the satellite transitions within the Swan system shows that they may be competitive with the intercombination transitions. GvDB's study of fluorescent emission by cometary C_2 molecules further assumes that the cometary gas and dust cloud is optically thin at all relevant wavelengths (line as well as continuum) and that the solar photons control the C_2 level populations without the assistance of collisions between the C_2 and cometary atoms and molecules. Our discussion (below) of optical depth effects and the contributions of collisions suggests that neither are responsible for the unexpectedly high populations of low-J levels.

Since the different behavior of F_1, F_2, and F_3 at low J reflects fundamental characteristics of the rates of the intercombination transitions and since the magnitude of the transition probabilities, especially that of the leading $a \leftrightarrow X$ transition, is known from calculations and by reference to the heliocentric variation of the Swan band ratio R, it would appear that, if agreement at low J is to be achieved under the general conditions assumed by GvDB, new radiative processes must be invoked. We considered the role of the satellite transitions of the Swan bands. These transitions, which were not considered by GvDB, occur between the substates F_1, F_2, and F_3 with approximately equal transition probabilities for $F_1 \leftrightarrow F_2$, and $F_2 \leftrightarrow F_3$ and with transition probabilities that are largest at the band origins. Our interest in the satellite transitions was stimulated by the realization that they may occur at a rate that is competitive with the $a \leftrightarrow X$ rates and so maintain approximately equal populations in F_1, F_2, and F_3. Rough estimates of various rates for the population and depopulation of a $^3\Pi_u$ ($v = 0$) are sketched in Figure 12. The dominant rates arise from transitions within the Swan system. We give in Figure 12 estimates of the rates at a heliocentric distance of 1 AU for excitation from $v'' = 0$ with a return to any level except the starting level ($0 \rightarrow$ all) and to $v'' = 0$ with a change of rotational level ($0 \rightarrow 0$). Rates into $v'' = 0$ are given for initial vibra-

© American Astronomical Society • Provided by the NASA Astrophysics Data System

1990ApJ...353..640L

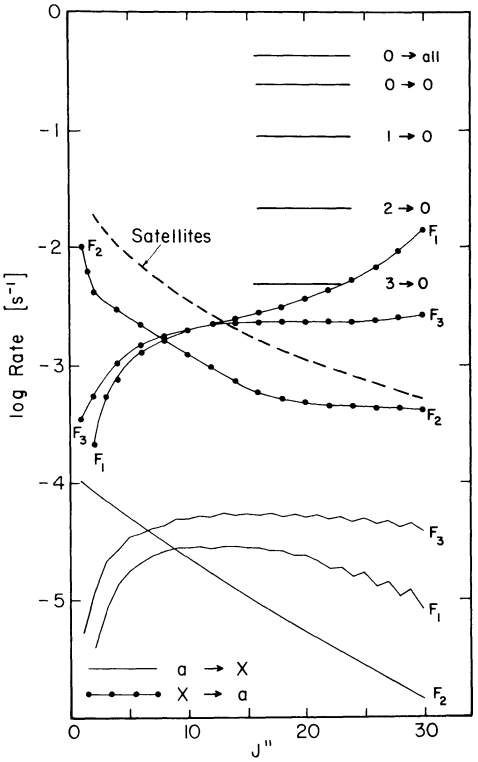

FIG. 12.—Rates of population and depopulation for rotational levels of $a\ ^3\Pi_u (v = 0)$. See text.

tional levels $v'' = 1, 2, 3$ (see the labels $1 \rightarrow 0$, $2 \rightarrow 0$, and $3 \rightarrow 0$ in Fig. 12); these rates which are only weakly dependent on the rotational level are expressed per unit population in $v'' = 0$, and the relative populations of the vibrational levels are estimated using the vibrational temperature given by GvDB. The rate for a transfer between spin substates (i.e., satellite transitions), $F_1 \leftrightarrow F_2$ or $F_2 \leftrightarrow F_3$ is given for the process $a(v = 0) \rightarrow d(v') \rightarrow a(v = 0)$. The total rate for these transfers is larger by about a factor of about 1.5 due to processes $a(v = 0) \rightarrow d(v') \rightarrow a(v \neq 0)$.

Two collections of rates are shown for the a–X transitions. The probabilities for spontaneous emission from $a\ ^3\Pi_u (v = 0)$ to $X\ ^1\Sigma_g^+ (v = 0)$ are very small; we give the values computed by Le Bourlot and Roueff (1986). Rates for the population of $a\ ^3\Pi_u (v = 0)$ by spontaneous emission from $X\ ^1\Sigma_g^+ (v \geq 1)$ are estimated using the predicted vibrational temperature and an assumption that the total population in $a\ ^3\Pi_u$ is about a factor of 6 greater than that in $X\ ^1\Sigma_g^+$. This latter value was estimated by us from observations of the Ballik-Ramsay and Phillips systems in comet West 1976 VI and of the Swan and Mulliken systems in comet Bradfield 1979 X.

Inspection of Figure 12 shows that the satellite transitions at low J contribute at a rate exceeding those arising from the $a \leftrightarrow X$ transitions. However, there are indirect contributions of the $a \leftrightarrow X$ transitions to be considered; for example, these transitions may be relatively more important for excited vibrational levels of $a\ ^3\Pi_u$ that are linked to $v'' = 0$ through the Swan (and Ballik-Ramsay) system. Our comparison of rates ignores the c–X transition and uses Le Bourlot and Roueff's rates for the a–X transition. GvDB remark that the latter correspond to $|R_e|^2_{aX} \sim 1 \times 10^{-6}$, but $|R_e|^2_{aX} \sim 3.5 \times 10^{-6}$ is needed to fit the high-resolution spectra. With the larger $|R_e|^2_{aX}$, the apparent role of the satellite transitions is diminished.

We suggest that satellite transitions among low rotational levels effect $F_1 \leftrightarrow F_2$ and $F_2 \leftrightarrow F_3$ transitions at such a rate that the differences in the F_1, F_2, and F_3 populations arising from the distinct dependence of $a \leftrightarrow X$ rates on spin substate are erased. The total population of the low-J levels may remain controlled by the $a \leftrightarrow X$ transitions. Our suggestion is readily testable by adding the satellite transitions in the Swan and Ballik-Ramsay systems to the matrix of rates previously considered by GvDB.

GvDB, who observed that the lower rotational levels are more highly populated in the coma than in the nucleus, proposed that the change of rotational excitation was the result of shielding of the solar photons by cometary dust particles; i.e., the intercombination transitions assume a greater role in setting the statistical equilibrium of the C_2 molecules. A satisfactory fit to the spectrum of the nucleus was achieved for an optical depth $\tau_v \approx 0.8$ in the visible. Estimates of the optical depth due to dust suggest that the comet was quite optically thin, say, $\tau_v < 0.01$ (O'Dell *et al.* 1988). GvDB noted O'Dell *et al.*'s estimate of τ_v and considered that the proposal of shielding "may be untenable." Moreover, shielding that enhances the role of the intercombination transitions will not reconcile the predicted and observed low-J populations.

The estimated temperature of 190 K for the cold sample of C_2 molecules is close to the expected kinetic temperature for gas molecules in the comet. If collisions between molecules were to be competitive with the rates of fluorescent excitation, the C_2 molecules would achieve a low rotational temperature. Such a simple explanation for the low rotational temperature of the low-J levels fails because the gas densities are too low. GvDB estimated that collisional and fluorescent excitation are comparable for particle densities $n \sim 10^{10}$ cm^{-3} and that such densities may be found only within about 100 km of the nucleus. Since C_2 is formed from molecules with scale lengths much greater than 100 km, the C_2 molecules inhabit regions of the coma where the particle densities are too small for collisional excitation to be effective. In Figure 13, we show the relative radial density dependence of grandparent (here C_2H_2),

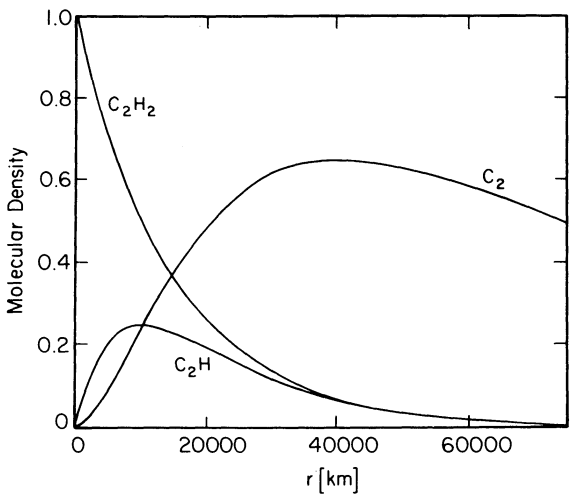

FIG. 13.—The radial dependence of the relative densities (molecules cm^{-3}) of the C_2 grandparent (here, labeled C_2H_2), parent (here, C_2H), and C_2. A Haser model is assumed with the scale lengths taken from O'Dell *et al.* (1988).

© American Astronomical Society • Provided by the NASA Astrophysics Data System

1990ApJ...353..640L

parent (here C_2H), and C_2 according to the scale lengths estimated by O'Dell *et al.* (1988). It is apparent that only a trace amount of C_2 is formed within the inner 100 km where collisions may outpace excitation by the sunlight. At the radial distance at which the C_2 is a maximum, the gas density was 10^4–10^5 cm^{-3} according to spacecraft measurements (Kim, A'Hearn, and Cochran 1989). At such densities, collisional excitation is completely negligible.

Our final suggestion for the origin of the rotationally cold low-J' molecules is that these molecules are freshly formed molecules observed before they have been driven into equilibrium by fluorescence in the sunlight. This suggestion about the origins of the cold low-J' molecules must pass at least two simple tests: (1) there must be an adequate number of freshly formed molecules; (2) the parent of C_2 must be photodissociated such that the low-J' C_2 molecules are rotationally cold.

An estimate of the number of freshly formed molecules is readily obtained from Haser's model using the scale lengths estimated by O'Dell *et al.* for the grandparent, parent, and C_2 molecules. For the model that gives the radial density gradients shown in Figure 13, we give in Figure 14 the column densities as a function of projected distance from the comet's nucleus and as a function of the maximum time (τ) since formation of the C_2 molecule. Since the C_2 molecules are expected to attain equilibrium in sunlight in about 500 s, the observed sample of freshly formed molecules is required to be consistent with that predicted for $\tau < 500$ s. Since our estimate (see bar on Fig. 14) that the low T_{rot} molecules constitute a few percent of the total sample along a line of sight close to the nucleus corresponds to $\tau \sim 100$ s, the test for consistency is passed successfully. Furthermore, the fractional population of freshly formed molecules is observed, as predicted, to decline with increasing projected distance from the nucleus.

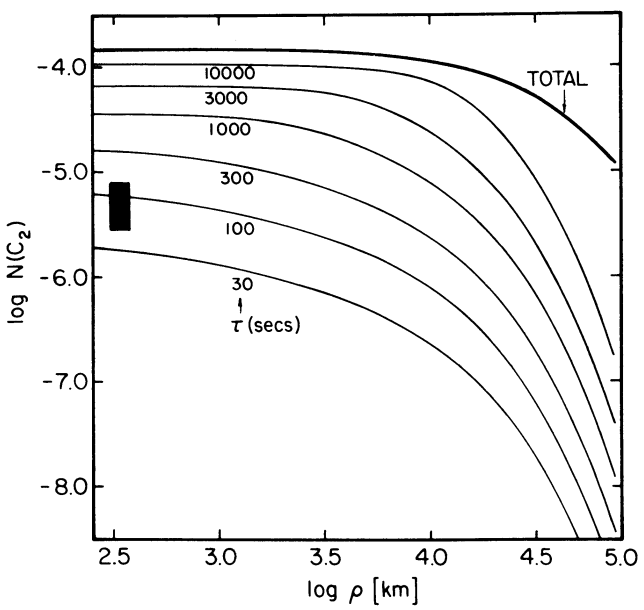

FIG. 14.—The variation with projected distance (ρ) of the C_2 column density (in arbitrary units). The thick line shows the total column density computed for the Haser model with scale lengths taken from O'Dell *et al.* (1988). The light lines show the column densities of freshly formed molecules, where τ is the maximum time (in seconds) since formation of the molecule. The bar shows the range of estimates for the observed fractional population of the low-J' molecules.

There are indications from laboratory studies of the photodissociation of C_2H_2 and C_2H that C_2 molecules can be formed abundantly in low-J' levels with a low rotational temperature. Acetylene (C_2H_2) is a likely candidate for the grandparent of C_2 with the C_2H radical, an intermediate product from photodissociation of C_2H_2, as the C_2 molecule's parent. Fletcher and Leone (1989) showed that room temperature C_2H_2 molecules when photodissociated (at 1930 Å) are rotationally cooled. Cometary C_2H_2 molecules are expected to be rotationally cold because C_2H_2 has no strong electronic transitions that can populate the rotational ladder by fluorescence. For the same reason, the C_2H radicals seem unlikely to be rotationally excited before they are photodissociated. Urdahl, Bao, and Jackson (1988) show that the C_2 ($A\ ^1\Pi_u$) molecules resulting from photodissociation of C_2H with C_2H_2 as the initial gas are vibrationally cold with a rotational population that resembles that reported here for comet Halley. The laboratory investigation of the vibrationally cold C_2 ($a\ ^3\Pi_u$) products is incomplete, but their rotational population appears to resemble that for C_2 ($A\ ^1\Pi_u$) for which the low-J' and high-J' products have rotational temperatures $T_{rot} \simeq 100$ K and 1200 K, respectively (Jackson 1989). The former is similar to our observed estimate (190 K). The high-J' products are presumably masked by the dominant population of C_2 molecules in fluorescence equilibrium. Our comparison of spectra taken on and off the nucleus did suggest changes in the high-J' populations that could be due to a changing mixture of freshly-formed and mature C_2 molecules. Jackson (1989) notes that similar bimodal populations for $A\ ^1\Pi_u$ are produced from photodissociation of C_2H_2, C_2D_2, and CF_3C_2H. This similarity suggests that the identification of the low-J' population with freshly formed C_2 molecules need not be linked to a specific parent molecule for C_2.

Although our suggestion that the low-J' sample is contaminated by freshly formed C_2 molecules passes the two tests listed above, it is not entirely clear why the observations in Figure 4 form such a tightly defined Boltzmann distribution. One expects the contributions from molecules over the entire gamut from freshly formed to fluorescence equilibrium to result in a smearing of the Boltzmann distribution. For this reason, we suggest that the low-J' sample is dominated by molecules in equilibrium with the satellite transitions exerting a major influence.

The C_2 $d\ ^3\Pi_g$ vibrational temperature as monitored by the Swan band ratio $F(\Delta v = +1)/F(\Delta v = 0)$ increases for nucleocentric distances less than 5000 km (O'Dell *et al.* 1988; Vanysek, Valníček, and Sudová 1988). This increase was ascribed by O'Dell *et al.* to a greater preponderance of freshly formed C_2 molecules close to the nucleus. Laboratory experiments have yet to characterize the vibrational populations of C_2 molecules formed by photodissociation of likely parent molecules such as C_2H. However, if preliminary indications that the vibrational temperature is low are confirmed, alternative explanations will have to be sought for the increase in the band ratio toward the nucleus.

V. CONCLUDING REMARKS

Our rotational analysis of the intensities of the C_2 Swan 0–0 band's emission lines in spectra of comet Halley has been compared with predictions of a refined calculation of the rotational populations achieved when cometary C_2 molecules achieve fluorescence equilibrium in sunlight. Such a comparison shows that observed and predicted populations for levels with $J' \gtrsim 15$

© American Astronomical Society • Provided by the NASA Astrophysics Data System

1990ApJ...353..640L

are in good agreement. This agreement is to be contrasted with the situation for the low rotational levels ($J' < 15$) for which our observations show that the F_1, F_2, and F_3 levels define a single Boltzmann distribution at a low rotational temperature, but the F_1, F_2, and F_3 levels are predicted to reach distinctly different populations. This discrepancy was not fully resolved, but it appears likely that the satellite transitions within the Swan bands may be a key factor in establishing equilibrium populations for the low rotational levels. For the satellite transitions to play a determining role, the a–X transition probabilities cannot be significantly greater than the values computed by Le Bourlot and Roueff (1986). Contributions from freshly formed C_2 molecules to the observed spectrum may account in part for the discrepancy.

At the earliest opportunity, expanded surveys of C_2 emission lines in bright comets need to be pursued. With the increasing availability of echelle spectrometers capable of recording spectra over a broad bandpass, it should be possible to extend the spectral analysis reported here to many bands and several band sequences of the Swan system as well as to the Phillips system. Since relative contributions of the strong, satellite, and intercombination transitions to the equilibrium populations vary with heliocentric distance, spectra should be obtained over a broad range in heliocentric distances and at varying distances from the nucleus of comets of differing dust content. The level populations derived from such spectra will represent a stiff challenge for predictions of the emission spectrum from cometary C_2 molecules.

We are most grateful to R. Gredel who sent us a magnetic tape containing detailed predictions of the C_2 level populations for a variety of cases, and to J. Le Bourlot and E. Roueff who provided a detailed listing of their predicted transition probabilities for the a–X intercombination transition. We thank A. Cochran, R. F. Curl, W. M. Jackson, and C. R. O'Dell for helpful discussions. A. C. D. wishes to thank NOAO for a travel grant and the AAS for partial support through the small grants program. We wish to thank M. C. Bories for computing assistance.

REFERENCES

Amiot, C. 1983, *Ap. J. Suppl.*, **52**, 329.
Appenzeller, I., and Münch, G. 1987, *Astr. Ap.*, **187**, 465 (AM).
Bauer, W., Becker, K. H., Bielefeld, M., and Meuser, R. 1986, *Chem. Phys. Letters*, **123**, 33.
Bauer, W., Becker, K. H., Hubrich, C., Meuser, R., and Wildt, J. 1985, *Ap. J.*, **296**, 758.
Beisser, K., Boenhardt, H., Vanysek, V., Reinsch, K., Grün, E., and Massonne, L. 1989, *Messenger*, No. 56.
Callomon, J. H., and Gilby, A. C. 1963, *Canadian J. Phys.*, **41**, 995.
Dressler, K., and Ramsay, D. A. 1959, *Phil. Trans. Roy. Soc. London, A*, **251**, 553.
Dwivedi, P. H., Branch, D., Huffaker, J. N., and Bell, R. A. 1978, *Ap. J. Suppl.*, **36**, 573.
Fletcher, T. R., and Leone, S. R. 1989, *J. Chem. Phys.*, **90**, 871.
Gredel, R., van Dishoeck, E. F., and Black, J. H. 1989, *Ap. J.*, **338**, 1047 (GvDB).
Haser, L. 1957, *Bull. Acad. Roy. de Belgique, Class des Sci., 5th Ser.*, **43**, 740.
Jackson, W. M. 1989, private communication.
Kim, S. J., A'Hearn, M. F., and Cochran, W. D. 1989, *Icarus*, **77**, 98.
Krishna Swamy, K. S., and O'Dell, C. R. 1977, *Ap. J.*, **216**, 158.
———. 1979, *Ap. J.*, **231**, 624.
———. 1981, *Ap. J.*, **251**, 805.
———. 1987, *Ap. J.*, **317**, 543.
Lambert, D. L., and Danks, A. C. 1983, *Ap. J.*, **268**, 428 (LD).
Le Bourlot, J., and Roueff, E. 1986, *J. Molec. Spectrosc.*, **120**, 157.
O'Dell, C. R., Robinson, R. R., Krishna Swamy, K. S., McCarthy, P. J., and Spinrad, H. 1988, *Ap. J.*, **334**, 476.
O'Neil, S. V., Rosmus, P., and Werner, H.-J. 1987, *J. Chem. Phys.*, **87**, 2847.
Phillips, J. G. 1968, *J. Molec. Spectrosc.*, **28**, 233.
Urdahl, R. S., Bao, Y., and Jackson, W. M. 1988, *Chem. Phys. Letters*, **152**, 485.
van Dishoeck, E. F. 1983, *J. Chem. Phys.*, **77**, 277.
Vanysek, V., Valníček, B., and Sudová, J. 1988, *Nature*, **333**, 435.
Whiting, E. E. 1973, NASA Tech. Note, D-7268.

C. Arpigny and P. Magain: Institut d'Astrophysique, Université de Liège, B-4200, Ougrée-Liège, Belgium

A. C. Danks: Applied Research Corporation, 8201 Corporate Drive, Landover, MD 20785

D. L. Lambert and Y. Sheffer: Department of Astronomy, University of Texas, Austin, TX 78712

© American Astronomical Society • Provided by the NASA Astrophysics Data System